Evolution of Dispersal Rates in Metapopulation Models: Branching and Cyclic Dynamics in Phenotype Space

Michael Doebeli; Graeme D. Ruxton

Evolution, Vol. 51, No. 6 (Dec., 1997), 1730-1741.

Stable URL:
http://links.jstor.org/sici?sici=0014-3820%28199712%2951%3A6%3C1730%3AEODRIM%3E2.0.CO%3B2-1

Evolution is currently published by Society for the Study of Evolution.

Evolution, 51(6), 1997, pp. 1730–1741

EVOLUTION OF DISPERSAL RATES IN METAPOPULATION MODELS: BRANCHING AND CYCLIC DYNAMICS IN PHENOTYPE SPACE

MICHAEL DOEBELI[1] AND GRAEME D. RUXTON[2]
[1] *Zoology Institute, University of Basel, Rheinsprung 9, CH-4051 Basel, Switzerland*
email: doebeli@ubaclu.unibas.ch
[2] *Division of Environmental and Evolutionary Biology, Graham Kerr Building, University of Glasgow, Glasgow G12 8QQ, UK*
email: gdr1m@udcf.gla.ac.uk

Abstract.—We study the evolution of dispersal rates in a two patch metapopulation model. The local dynamics in each patch are given by difference equations, which, together with the rate of dispersal between the patches, determine the ecological dynamics of the metapopulation. We assume that phenotypes are given by their dispersal rate. The evolutionary dynamics in phenotype space are determined by invasion exponents, which describe whether a mutant can invade a given resident population. If the resident metapopulation is at a stable equilibrium, then selection on dispersal rates is neutral if the population sizes in the two patches are the same, while selection drives dispersal rates to zero if the local abundances are different. With non-equilibrium metapopulation dynamics, non-zero dispersal rates can be maintained by selection. In this case, and if the patches are ecologically identical, dispersal rates always evolve to values which induce synchronized metapopulation dynamics. If the patches are ecologically different, evolutionary branching into two coexisting dispersal phenotypes can be observed. Such branching can happen repeatedly, leading to polymorphisms with more than two phenotypes. If there is a cost to dispersal, evolutionary cycling in phenotype space can occur due to the dependence of selection pressures on the ecological attractor of the resident population, or because phenotypic branching alternates with the extinction of one of the branches. Our results extend those of Holt and McPeek (1996), and suggest that phenotypic branching is an important evolutionary process. This process may be relevant for sympatric speciation.

Key words:—Adaptive dynamics, coexistence, complex population dynamics, evolutionary cycling, invasion exponents, polymorphism, sympatric speciation.

Received December 13, 1996. Accepted June 16, 1997.

Traditional evolutionary theory is an equilibrium theory. Optimality models as well as game theoretic evolutionary models involve the search for phenotypes which cannot be replaced by other phenotypes and hence represent an evolutionary equilibrium. Despite the success of such models (Maynard Smith 1982; Stearns 1992; Roff 1992), just as in ecological theory there is a need to extend evolutionary theory beyond the equilibrium concept. For example, evolutionary stable strategies are always equilibria for the corresponding evolutionary dynamics, but in many cases these equilibria may be unstable, so that populations that are close to an evolutionary stable strategy evolve away from it instead of towards it (Cressman 1992). A typical situation where equilibrium theory may fail to capture the essence of an evolutionary process occurs when there is an interaction between ecological and evolutionary dynamics. Often a trait whose evolution is to be studied affects the ecological dynamics of a population, and the population dynamics in turn determine the selection pressures on the trait. This can lead to eco-evolutionary feedback mechanisms which result in non-equilibrium evolutionary dynamics.

Here we provide explicit examples for some of the basic features of non-equilibrium evolutionary dynamics. These examples involve the evolution of dispersal rates in metapopulation models and include phenomena such as evolutionary cycling in phenotype space and evolutionary branching, in which a phenotypic lineage becomes polymorphic and splits into two coexisting phenotypic branches. Our work is an extension of the pioneering work by McPeek and Holt (1992) and Holt and McPeek (1996), who studied the evolution of dispersal rates in a two patch metapopulation. Holt and McPeek (1996) argued that if the patches have different carrying capacities and if the local dynamics are chaotic, then there can be selection for high dispersal rates. In addition, they showed that different dispersal rate phenotypes could coexist. We extend these results and put them into the framework of invasion exponents (Metz et al. 1992; Rand et al. 1994) and adaptive dynamics (Metz et al. 1996, Geritz et al. 1997).

An invasion exponent describes in very general terms the invasion success of a mutant phenotype whose environment is determined on the one hand by the fixed biotic and abiotic constraints of the problem, which are the same for all phenotypes, and on the other hand by certain aspects of the resident population, e.g., its phenotypic composition or its population dynamics. Technically, the invasion exponent is the logarithm of the long-term growth rate of a mutant in an environment given by the resident population, and a mutant can invade if and only if its invasion exponent is larger than zero. The invasion exponent is the main tool in the theory of adaptive dynamics proposed by Hans Metz and his colleagues (Metz et al. 1996; Geritz et al. 1997). These authors attempt to develop a general theory for evolutionary dynamics in multidimensional phenotype spaces, much like the bifurcation theory for "ordinary" dynamical systems. We view our results as a case study for this theory of adaptive dynamics.

After introducing the model and the numerical methods in the next section, we begin the results section by considering a metapopulation consisting of two identical patches. In this case, non-zero dispersal rates evolve if the metapopulation exhibits non-equilibrium ecological dynamics. Depending on the dispersal rate, the metapopulation has qualitatively different population dynamic attractors, and the direction of

selection can depend on the attractor on which the resident is moving. This can lead to evolutionary cycling of dispersal rates. In contrast to the equal patch case where it cannot be observed, phenotypic branching is a likely outcome of the evolutionary dynamics when the patches are ecologically different. Branching can occur when the system exhibits nonequilibrium (e.g., cyclic) population dynamics, and repeated branching is possible. In addition, if there is a cost to dispersal, evolutionary branching can alternate with the extinction of one of the branches, which again results in cyclic evolutionary dynamics in phenotype space. Finally, in the discussion we point out some differences between the results of Holt and McPeek (1996) and our results, and we discuss the potential significance of evolutionary branching for sympatric speciation.

Model and Numerical Methods

Our metapopulation model is based on difference equations

$$N_{t+1} = N_t f(N_t), \tag{1}$$

where N_t is the population size at time t, and $f(N)$ is the density dependent fitness function, i.e., the reproductive output per individual. Here we work with the fitness function of Maynard Smith and Slatkin (1973):

$$f(N) = \frac{\lambda}{1 + (aN)^b}. \tag{2}$$

This model is more suitable for ecological and evolutionary problems than other equations such as the Ricker equation (Ricker 1954) or Hassell's (1975) equation, because the function given by (2) has an inflection point, in contrast to the corresponding functions in Ricker's or Hassell's model (see also Doebeli 1995; Blarer and Doebeli 1996). However, the results reported here do not depend crucially on the choice of the basic difference equation, and similar results can be obtained with other models, e.g., those in Bellows (1981).

In eq. (2), λ is the intrinsic growth rate of the population, i.e., the number of offspring per individual when there are no density-dependent effects of competition. The parameter b reflects the type and strength of the competition that leads to density dependence, and the parameter a scales the carrying capacity of the population (Bellows 1981). The carrying capacity N^* is defined by $f(N^*) = 1$, and hence is an equilibrium for the dynamic process described by (1). As is well known, the stability of this equilibrium is determined by the slope c of $N \cdot f(N)$ at N^*. Clearly,

$$N^* = \frac{(\lambda - 1)^{1/b}}{a}, \tag{3}$$

and

$$c = 1 - b\frac{\lambda - 1}{\lambda}. \tag{4}$$

If $|c| < 1$, N^* is locally stable, and as $|c|$ increases above 1, the system exhibits the period-doubling route to chaos (May and Oster 1976).

We extend model (1) to a two patch model by assuming that in each patch and in each generation, reproductive dynamics given by (1) are followed by dispersal to the other patch. We denote the population size at time t in patch 1 by N_t, and that in patch 2 by M_t. Then after reproduction, but before dispersal, the population sizes are

$$\begin{aligned} \tilde{N}_t &= N_t \cdot f(N_t) \\ \tilde{M}_t &= M_t \cdot g(M_t), \end{aligned} \tag{5}$$

where f and g are the fitness functions in the two patches. They are both of the general form (2), but the parameter values may differ in the two patches, in which case the patches are ecologically different. After reproduction, a fraction d of each local population moves to the other patch, where $0 \le d \le 1$. The parameter d can be interpreted as the probability that an individual born in one of the patches moves to the other patch. After dispersal, i.e., at the start of the next generation, the population sizes in the two patches are

$$\begin{aligned} N_{t+1} &= (1 - d)\cdot\tilde{N}_t + d\cdot\tilde{M}_t \\ &= (1 - d)\cdot N_t \cdot f(N_t) + d\cdot M_t \cdot g(M_t) \\ M_{t+1} &= (1 - d)\cdot\tilde{M}_t + d\cdot\tilde{N}_t \\ &= (1 - d)\cdot M_t \cdot g(M_t) + d\cdot N_t \cdot f(N_t). \end{aligned} \tag{6}$$

System (6) specifies the dynamics of the two patch metapopulation model. In matrix form, it is written as

$$\begin{pmatrix} N_{t+1} \\ M_{t+1} \end{pmatrix} = A(N_t, M_t, d)\cdot\begin{pmatrix} N_t \\ M_t \end{pmatrix}, \tag{7}$$

where $A(N_t, M_t, d)$ is the matrix

$$A(N_t, M_t, d) = \begin{pmatrix} (1 - d)\cdot f(N_t) & d\cdot g(M_t) \\ d\cdot f(N_t) & (1 - d)\cdot g(M_t) \end{pmatrix}. \tag{8}$$

To study the evolution of dispersal, we define a dispersal phenotype as given by a dispersal rate d. Suppose that, given a population consisting of a resident phenotype d, a rare mutant d^{mut} appears in the population. By assumption, the mutant has the same reproductive fitness functions as the resident. Since the mutant is rare, the local reproductive output of the mutant in each patch is determined by the resident densities. Therefore, the dynamics of the mutant vector (N_t^{mut}, M_t^{mut}) are determined by the matrices $A(N_t, M_t, d^{mut})$, i.e., given by

$$\begin{pmatrix} N_{t+1}^{mut} \\ M_{t+1}^{mut} \end{pmatrix} = A(N_t, M_t, d^{mut})\cdot\begin{pmatrix} N_t^{mut} \\ M_t^{mut} \end{pmatrix}, \tag{9}$$

where $\{N_t, M_t\}_{t=0}^{\infty}$ is the time series of the resident. It follows (e.g., Metz et al. 1992) that the long term growth rate of the mutant d^{mut} in the resident d is the T-th root of the dominant eigenvalue of the product of $A(N_t, M_t, d^{mut})$ over T time steps, where T goes to infinity. The invasion exponent $p(d, d^{mut})$ is defined as the logarithm of this long-term growth rate:

$$\rho(d, d^{mut}) = \lim_{T\to\infty}\frac{1}{T}\ln\left[\left|\prod_{t=1}^{T} A(N_t, M_t, d^{mut})\right|\right], \tag{10}$$

where the notation $|B|$ denotes the dominant eigenvalue of a matrix B. The mutant d^{mut} can invade the resident d if and only if

$$\rho(d, d^{mut}) > 0. \tag{11}$$

Note that the invasion exponent depends on the ecological time series of the resident. It is possible that for a given dispersal rate d, there are different population dynamic attractors of system (6) (Hastings 1993), leading to different resident time series. Thus, whether an invasion exponent is greater than zero may depend on the population dynamic attractor of the resident. This will be important later on.

Invasion exponents are the central object of study in the theory of adaptive dynamics proposed by Hans Metz and his collaborators (Metz et al. 1996; Geritz et al. 1997). Here we will use invasion exponents to construct invasion diagrams, in which different regions of a plane with the resident phenotypes as x-axis and the mutant phenotypes as y-axis are distinguished according to the sign of the invasion exponent $\rho(d, d^{mut})$ as a function of the coordinates (d, d^{mut}) in the resident-mutant plane. Such diagrams yield a qualitative representation of the evolutionary process.

Unfortunately, it is often impossible to calculate the invasion exponent (10) analytically, because the time series of the resident may be too complicated. To obtain invasion diagrams, we therefore use a numerical procedure that consists of simulating a four-dimensional system comprising the resident and the mutant densities in both patches. For this we assume that the fitness of both the resident and the mutant depends on the total density in a patch, i.e., on the sum of the densities of the resident and the mutant in that patch. Thus the resident dynamics become

$$\begin{aligned} N_{t+1} &= (1 - d)\cdot N_t \cdot f(N_t + N_t^{mut}) \\ &\quad + d\cdot M_t \cdot g(M_t + M_t^{mut}) \\ M_{t+1} &= (1 - d)\cdot M_t \cdot g(M_t + M_t^{mut}) \\ &\quad + d\cdot N_t \cdot f(N_t + N_t^{mut}), \end{aligned} \tag{12}$$

and the mutant dynamics are

$$\begin{aligned} N_{t+1}^{mut} &= (1 - d^{mut})\cdot N_t^{mut} \cdot f(N_t + N_t^{mut}) \\ &\quad + d^{mut}\cdot M_t^{mut} \cdot g(M_t + M_t^{mut}) \\ M_{t+1}^{mut} &= (1 - d^{mut})\cdot M_t^{mut} \cdot g(M_t + M_t^{mut}) \\ &\quad + d^{mut}\cdot N_t^{mut} \cdot f(N_t + N_t^{mut}). \end{aligned} \tag{13}$$

To see whether invasion of a mutant is possible, one runs (12) for a number of iterations with $N_t^{mut} = 0$ and $M_t^{mut} = 0$ to remove transient effects, then introduces a small amount of mutants at a certain time T and iterates eqs. (12) and (13) for a number of further iterations. Then, at some time $T + T_1$, the frequency of the mutant over the next few generations is recorded. If the average frequency over these generations is bigger than a certain threshold, then we set $\rho(d, d^{mut}) > 0$. This procedure was used to produce the invasion diagrams appearing later in this paper. For all diagrams, the transient time T after which the mutant is initialized was set to 1000, the invasion time T_1 over which the fate of the mutant was decided was set to 10,000, the trial time over which the frequency of the mutant was recorded was set to 200, and the invasion threshold was set to 0.001.

To determine long-term evolutionary dynamics of dispersal rates, we used a second numerical procedure, in which the full dynamics for each of a number of phenotypes was calculated. For this an array of phenotypes was kept, and the dynamics of each phenotype was described by two equations for its local density in each patch. These equations are determined by the dispersal rate of the phenotype and by the fitness functions, which were the same for all phenotypes in one patch. Again it was assumed that the fitness functions depended on the total density of the population in a patch. If there are r phenotypes in the population, this leads to the system of equations for $i = 1, \ldots, r$:

$$\begin{aligned} N_{t+1}^i &= (1 - d^i)\cdot N_t^i \cdot f\left(\sum_{j=1}^{r} N_t^j\right) + d^i \cdot M_t^i \cdot g\left(\sum_{j=1}^{r} M_t^j\right) \\ M_{t+1}^i &= (1 - d^i)\cdot M_t^i \cdot g\left(\sum_{j=1}^{r} M_t^j\right) + d^i \cdot N_t^i \cdot f\left(\sum_{j=1}^{r} N_t^j\right), \end{aligned} \tag{14}$$

where a superscript i indicates that the corresponding quantity is phenotype i specific. System (14) was iterated starting out with a single phenotype (i.e., $r = 1$). At the start of each generation, a new mutant phenotype appeared with probability equal to the mutation rate. If a new phenotype appeared, it was initialized at low densities in both patches, and the dimensionality of system (14) was increased by two (i.e., r was increased by one) for the ensuing iterations. At regular time intervals phenotypes that fell below a certain threshold density were considered extinct and removed from the population. By keeping track of the phenotypes that are present in the population, one can thus numerically follow the evolutionary dynamics of the dispersal rate. We always used a mutation rate of 0.005. If a mutation occurred, it was assumed that the new phenotype had mutated from one of the phenotypes already present in the population, which was selected with a probability that represented its frequency in the population (i.e., phenotype i was chosen as giving rise to the mutation with probability $(N_t^i + M_t^i)/\sum_{j=1}^{r} (N_t^j + M_t^j)$), and the mutant was then drawn from a Gaussian distribution with mean equal to the dispersal rate of the chosen resident phenotype and with standard deviation equal to 0.02. (If necessary, the corresponding random procedure was repeated until the dispersal rate of the mutant was in the feasible interval [0, 1].) While the results presented in the next section depend quantitatively on the numerical values for the mutation rate and the mutational variance, extensive numerical experiments suggest that the qualitative nature of the results is independent of these quantities.

Results

Equal Patches

We first assume that the patches are ecologically identical, i.e., that the fitness functions in the two patches are the same. Suppose that the local dynamics have a stable equilibrium. Then the coupled system (6) will also be at an equilibrium with the equilibrium population size in both patches being equal to N^*, equation (3) (Gyllenberg et al. 1993; Lloyd 1995). In particular, at equilibrium the fitness is the same in both patches (and equal to one). It is intuitively clear that in this situation there is no selection pressure on the dispersal rate. A mutant cannot gain by moving either less or more of its offspring between the patches, because the fitness, as de-

termined by the resident, is the same in both. Thus, dispersal is selectively neutral, and all invasion exponents are zero.

This simple case reflects a general fact: selection on dispersal rates is neutral whenever the resident dispersal rates are such that they lead to population dynamics such that at each time step the fitness is the same in both patches. In case the patches are equal, fitness in the two patches is the same if and only if the local populations are synchronized, i.e., if $N_t = M_t$. Such synchronized dynamics play a central role in the equal patch case: they determine the endpoint of the evolutionary dynamics of dispersal, as we shall see in a moment.

As the equilibrium of the local dynamics becomes unstable, attractors with non-synchronized dynamics start to appear in system (6) for very low as well as for very high dispersal rates d, while a range of intermediate dispersal rates tend to yield synchronized metapopulation dynamics (Hastings 1993; Gyllenberg et al. 1993, Lloyd 1995). Our extensive numerical work revealed two very clear trends: (1) if the resident dynamics are unsynchronized and the dispersal rate is low, then only mutants with higher dispersal rates than the resident can invade, (2) conversely, if the resident dynamics are unsynchronized and the dispersal rate is high, then only mutants with lower dispersal rates than the resident can invade. Both these trends persist until dispersal rates reach the intermediate range causing synchronized dynamics, where evolution of dispersal comes to a halt. These phenomena can occur with any type of non-equilibrium metapopulation dynamics, be they periodic or chaotic. They are comparable to results of McPeek and Holt (1992), who observed the evolution of intermediate dispersal rates when temporal fluctuations in fitness were driven extrinsically by parameter variation in metapopulations with two identical patches.

To be more clear about what we mean by unsynchronized dynamics, we discuss two typical cases. The first is a stable source-sink equilibrium that occurs for high dispersal rates despite possibly very complicated local dynamics (Doebeli 1995). In this equilibrium, one of the patches (the sink) has a very high population density, that is, fitness is very low in this patch, while the other patch (the source) is almost empty at the start of each generation. After reproducing, the situation is reversed due to the different fitness values in the two patches. But high dispersal then brings the system back to the original state at the start of the next generation. Doebeli (1995) proved that such source-sink equilibria are locally stable for a range of (high) dispersal rates. In a source-sink equilibrium, there is thus spatial heterogeneity in population abundance, but no temporal heterogeneity between generations. In such a situation, it can be shown, following the arguments in Hastings (1983) and Holt (1985), that a mutant can invade a resident if and only if the dispersal rate of the mutant is lower than that of the resident. Therefore, starting with dispersal rates leading to source-sink equilibria, evolution decreases dispersal. Then, for lower dispersal rates, synchronized attractors for the metapopulation dynamics start to appear and coexist with the source-sink attractor. As dispersal rates decrease further, the basin of attraction of the synchronized attractor increases, while that of the source-sink equilibrium decreases, until this equilibrium looses stability for low enough dispersal rates, and only the synchronized attractor is left, at which point selection on dispersal becomes neutral.

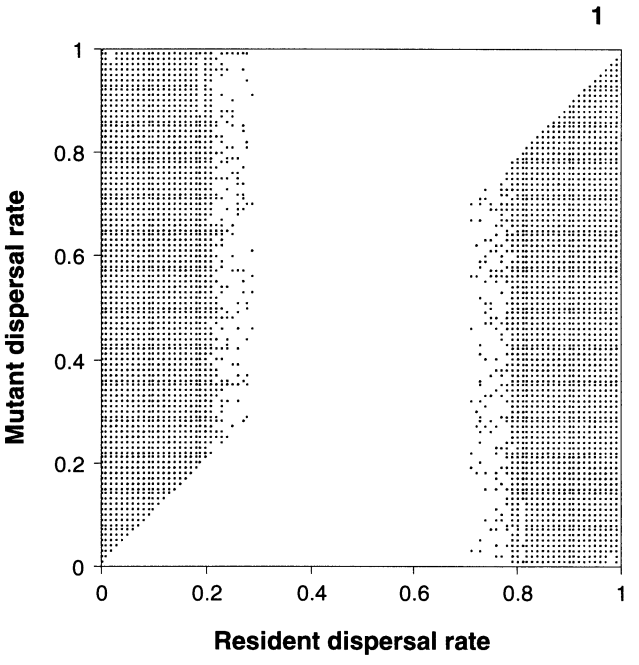

FIG. 1. Invasion diagram in the equal patch case. Low resident dispersal rates can only be invaded by higher mutants, and the opposite holds for very high resident dispersal. In the neutral region between circa 0.3 and 0.7 all invasion exponents are zero. The scatter of points at the borders of the neutral region indicates dependence of the invasion exponent on the population dynamic attractor of the resident. Here the invasion exponent is only > 0 if the random initial conditions used to initialize the resident lead to the asynchronous resident attractor. On the synchronous attractor invasion exponents are zero. The parameter values in the fitness function (2) were $\lambda = 4$, $a = 0.1$, and $b = 6.67$.

A similar but opposite process can happen for residents with low dispersal rates. With non-equilibrium local dynamics, such dispersal rates can lead to out-of-phase 2-cycles, in which the total population size remains constant, but the local populations alternate asynchronously between a high and a low density (Hastings 1993, Lloyd 1995). We show in the Appendix that such metapopulation dynamics induce selection for increased dispersal rates. Higher dispersal rates in turn lead to the existence of synchronized attractors (Gyllenberg et al. 1993), whose basins of attraction increase with increasing dispersal rates, whereas the basin of attraction of the out-of-phase 2-cycle decreases. Therefore, dispersal rates increase until again only the synchronized attractor is left, which is when evolution stops.

These phenomena are illustrated by the invasion diagram in Figure 1. For a set of equally spaced resident dispersal rates on the x-axis, the invasion exponent of mutant dispersal rates was calculated as described in section 2. If a mutant d^{mut} could invade a resident d, the pair (d, d^{mut}) was marked with a dot, otherwise this coordinate was left blank. Clearly, for very low resident dispersal rates only mutants with higher dispersal rates can invade, while the opposite is true for very high resident dispersal. For these dispersal rates the residents move on unsynchronized attractors. As resident dispersal

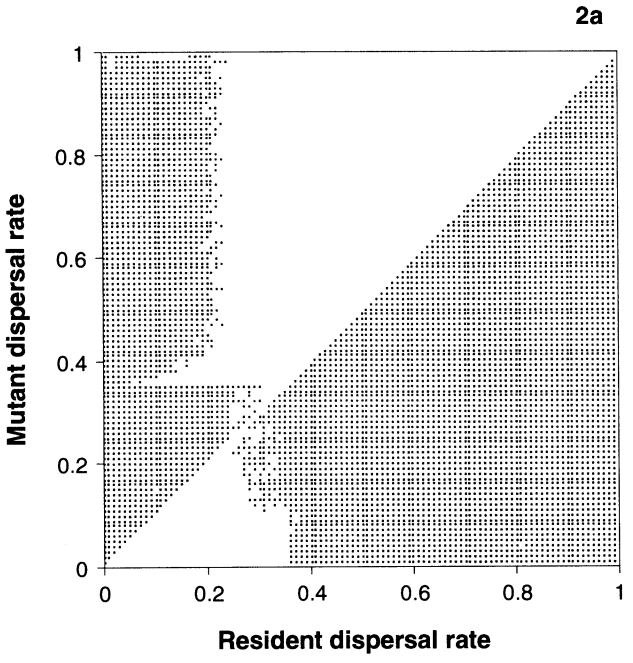

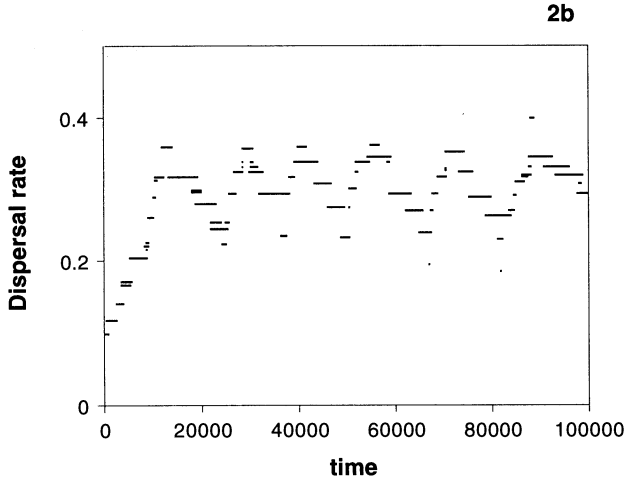

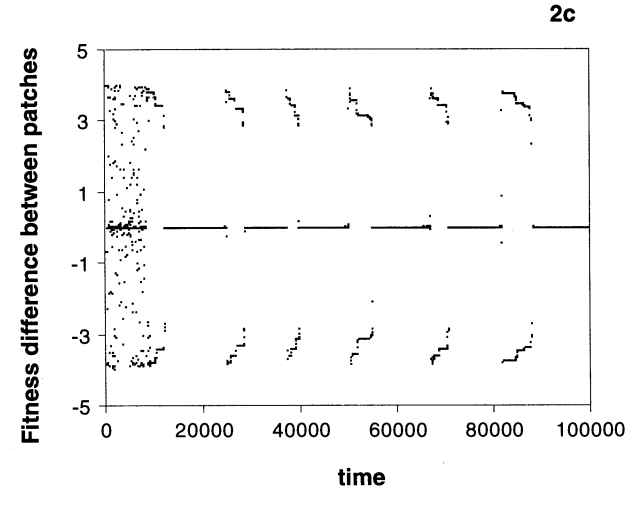

rates increase from low values respectively decrease from high values, these unsynchronized attractors coexist with synchronized attractors, and the basin of attraction of the synchronized attractor gets larger. Therefore, the chance that the random initial conditions used to calculate the time series of the resident and the invasion exponent are attracted by the synchronized attractor increases, so that the likelihood that an invasion exponent is greater than zero decreases. This can be seen by the less dense distribution of the dots marking positive invasion exponents in the regions of resident dispersal between circa 0.2 and 0.3 and between circa 0.7 and -0.8. Finally, for intermediate resident dispersal rates between circa 0.3 and 0.7, only the synchronized attractor is present, hence all invasion exponents are 0. The invasion diagram reflects that whether there is selection on dispersal may depend on the population dynamic attractor, and that evolution tends to move dispersal rates away from the extreme values 0 and 1 to the edges of an intermediate range of dispersal rates in which dispersal only evolves by drift.

To further illustrate the interaction between ecological and evolutionary dynamics, we incorporate a cost to dispersal in the metapopulation model by replacing system (6) with

$$N_{t+1} = (1 - d)\cdot N_t \cdot f(N_t) + d\cdot s\cdot M_t \cdot g(M_t)$$
$$M_{t+1} = (1 - d)\cdot M_t \cdot g(M_t) + d\cdot s\cdot N_t \cdot f(N_t). \quad (15)$$

Here s is the chance of a dispersing individual to survive the dispersal phase, which we assume to be the same for all phenotypes.

With a cost of dispersal, the region of selectively neutral dispersal rates in Figure 1 disappears. The corresponding invasion diagram is shown in Figure 2, in which everything is the same as in Figure 1, except that $s = 0.8$ in (15). Not only high resident dispersal rates, but also all resident dispersal rates that previously belonged to the neutral region can now be invaded by lower dispersal mutants. For low resident dispersal rates the selection for higher dispersal rates seen in Figure 1 is now counteracted by the cost of dispersal. Moreover, the relative strength of these opposing forces depends on the population dynamic attractor: if the resident is on a synchronized attractor, only the trend to decrease dispersal because of its cost is present. However, if the resident is on an unsynchronized attractor, selection for lower dispersal due to the cost is counteracted by the selection for higher dispersal due to unsynchronized dynamics (Appendix). For low resident dispersal rates, the latter force is stronger than the former, and higher dispersal mutants can invade.

←

FIG. 2. Effects of a cost to dispersal. Figure 2a is the same as Figure 1, except that $s = 0.8$ in (15). The neutral region disappears. The scatter of points between resident dispersal rates of circa 0.25 and 0.35 indicates dependence of invasion success on the resident attractor. This dependence leads to the evolutionary cycling shown in Figure 2b (see text). Here, at intervals of 25 time steps all dispersal phenotypes are shown whose frequency in the population is greater than five percent. In Figure 2c, every 25 time steps the difference between the fitness values in the two patches of the metapopulation is plotted. Synchronized dynamics correspond to zero difference and match the decreasing phases of the cycles in 2b.

This ecological dependence of the direction of selection is seen in the invasion diagram in Figure 2a as a region of resident dispersal rates between circa 0.25 and 0.35 which can be invaded by both lower and higher mutant dispersal rates, depending on which of the two coexisting population dynamic attractors the resident is moving.

The dependence of the selection pressure on population dynamics results in cyclic evolutionary dynamics of the dispersal rate, which is shown in Figure 2b. Here the evolutionary dynamics were started from a low dispersal rate corresponding to an unsynchronized attractor. Despite the cost, dispersal increases until it reaches values which induce synchronous dynamics. As soon as this happens, only the selective force due to the cost of dispersal is present, and dispersal starts to decrease. The decrease persists as long as the population remains on the synchronized attractor. Eventually, when dispersal rates are low enough, the system moves back to an attractor with unsynchronized dynamics, on which selection for higher dispersal kicks in again. The correspondence between the decreasing and the increasing parts of the resulting evolutionary cycle with synchronized and unsynchronized metapopulation dynamics is illustrated in Figure 2c, which shows the difference between the fitness values in the two patches as a function of time. Fitness differences of zero indicate synchronized dynamics, and these periods match the decreasing part of the cycles in Figure 2b, while the periods of unsynchronized dynamics with non-zero fitness differences match the increasing part of the cycles. Thus, a cost to dispersal can cause evolutionary cycling due to the dependence of the direction of selection on population dynamic attractors.

Unequal Patches

In this section we assume that the two patches in the metapopulation are ecologically different, i.e., that the fitness functions f and g in (6) are not the same. Up to now, the ecological dynamics of such systems have not been studied extensively, and such studies promise to be difficult. As an example of the dynamic complications that can arise, we note that with unequal patches it can happen that both local dynamics have a stable equilibrium when alone, but that the dynamics of the coupled metapopulation are chaotic (M. Doebeli, pers. obs.)! This is in stark contrast to the equal patch case, where local stable equilibrium dynamics always induce a stable equilibrium for the whole metapopulation (Rohani et al. 1996). However, here we simply want to present a few interesting evolutionary phenomena, without going into much population dynamic detail.

Assume first that the resident is at a stable equilibrium with constant local population sizes. Since the patches are unequal, the local equilibrium sizes are different, and hence there is spatial but no temporal heterogeneity in population abundance. As for the source-sink equilibrium in the equal patch case, it then follows that selection favors smaller dispersal rates. As a consequence, if successive replacements of residents by mutants with lower dispersal always lead to stable equilibrium dynamics, then the dispersal rate will evolve to zero. Thus, instead of being neutral over the whole range of dispersal rates as in the equal patch case, dispersal rates evolve to zero in the unequal patch case with equilibrium dynamics. (Note that no explicit cost to dispersal is assumed.)

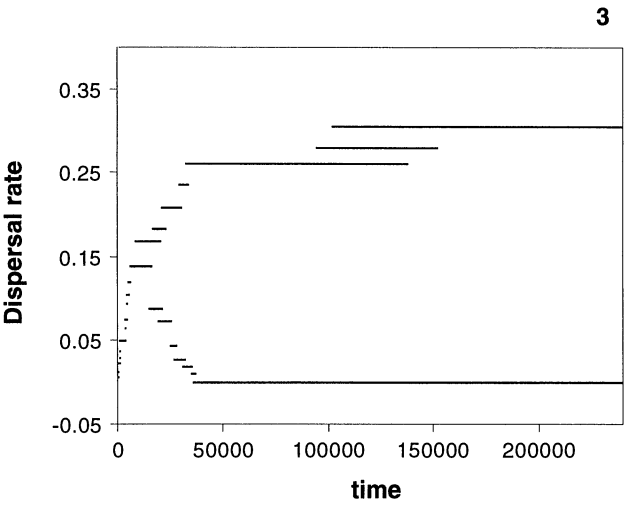

FIG. 3. Evolutionary branching of dispersal rates. Phenotypes with a frequency greater than five percent are plotted at intervals of 60 time steps. Branching occurs after circa 20,000 generations. At the evolutionary endpoint there are just two phenotypes with a frequency greater than five percent in the population. Their frequencies fluctuate, but are on average approximately equal. The parameter in the fitness functions in the two patches were: $a = 0.05$, $\lambda = 10$, and $b = 4.44$ in patch 1; $a = 0.1$, $\lambda = 10$, and $b = 4.44$ in patch 2. Thus patch 1 had twice the carrying capacity of patch 2.

This has also been noted by Holt and McPeek (1996), who argued that the same is true as long as the dynamics are not chaotic. They used the Ricker fitness function $f(N) = \lambda\exp[-aN]$ for their basic model. In this model the complexity is $c = 1 - \ln \lambda$, and the equilibrium density is $N^* = \ln \lambda/a$. Holt and McPeek (1996) considered patches that are different in their carrying capacity N^*, but not in their complexity, i.e., they assumed that the λ's are the same in the two patches, but that the a's are different. In our model, this would correspond to assuming equal λ's and b's, but unequal a's, cf. equations (3) and (4). If this is done, very similar results to those of Holt and McPeek (1996) are obtained: For complexities $|c|$ that do not lie in the chaotic region dispersal rates evolve to zero, and as complexities reach the chaotic region, non-zero dispersal rates can be maintained.

In addition, if $|c|$ is large enough, different dispersal phenotypes can coexist. Evolutionary dynamics resulting in such a polymorphism are shown in Figure 3. In this example, starting out from a very low dispersal rate of 0.005, dispersal first evolves to a value of circa 0.15, where it splits into two branches, one that evolves to zero and another that evolves to circa 0.3. Similar polymorphisms have been observed by McPeek and Holt (1992) in metapopulations with unequal patches in which fitness fluctuations were driven extrinsically by stochastic parameter variation. The intrinsic fluctuations in population dynamics during the evolutionary process shown in Figure 3 are always chaotic, as Holt and McPeek (1996) claimed to be necessary for polymorphisms in the deterministic case.

We extend the results of Holt and McPeek (1996) by as-

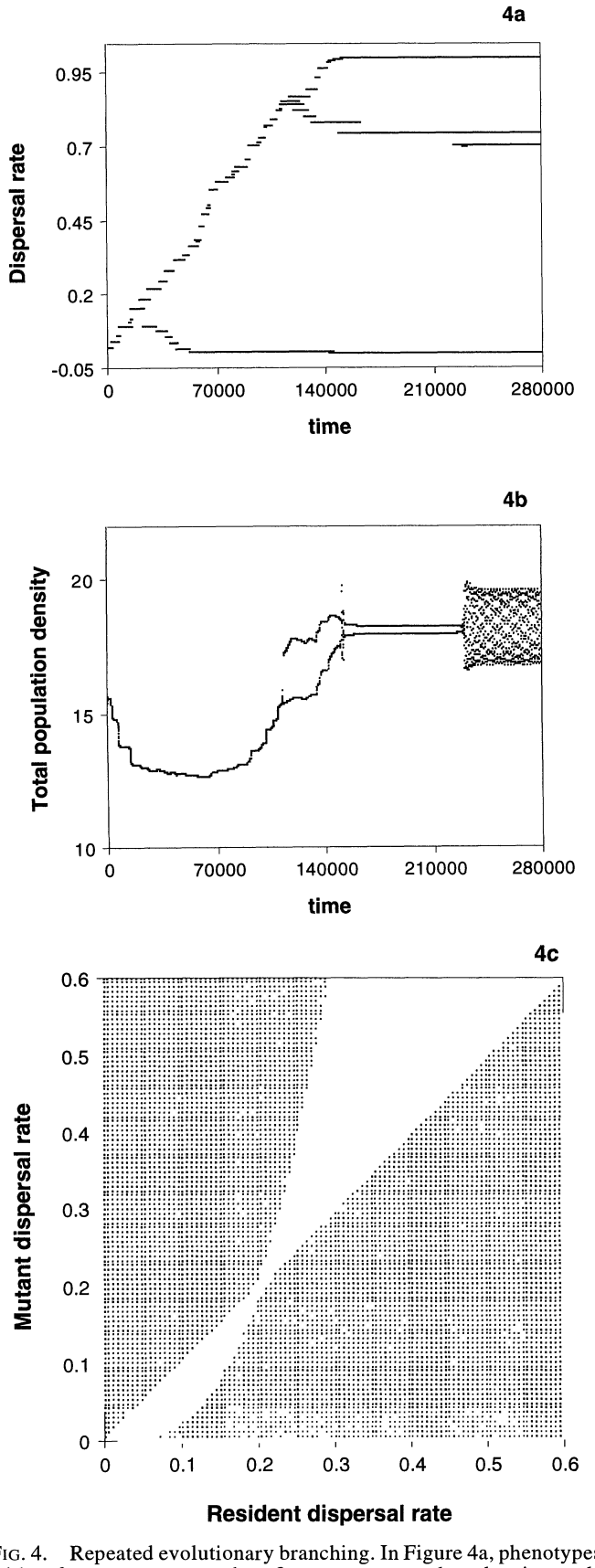

FIG. 4. Repeated evolutionary branching. In Figure 4a, phenotypes with a frequency greater than five percent are plotted at intervals of 70 time steps. After the initial branching at circa generation 20,000, the upper branch splits again at circa generation 120,000. At the evolutionary endpoint, there are three strains of dispersal rates present in the population. Again, their frequencies fluctuate, but are on average approximately equal. Figure 4b shows the metapopulation dynamics with the same time resolution. In the beginning the metapopulation is on a 2-cycle. Only one point of the cycle can be seen, because population size was plotted only every seventieth generation. Eventually, the 2-cycle changes into a 4-cycle (of which only two points can be seen), which, after being briefly interrupted by a period of complex dynamics, assumes a more constant form as the three dispersal branches become established. At circa generation 235,000, the middle branch becomes polymorphic, which induces what appear to be quasi-periodic population dynamics. Figure 4c is the corresponding invasion diagram. The angles that the + region forms with the 0-isoclines of the invasion exponent are much larger than 90 degrees (cf. Fig. 5). The parameter values were: $a = 0.1$, $\lambda = 3$, and $b = 2.925$ in patch 1; $a = 0.1$, $\lambda = 9$, and $b = 2.925$ in patch 2.

suming that the patches differ not only in their carrying capacity, but also in their intrinsic growth rates. This can be achieved by assuming that the a's and the b's are the same in the two patches, but that the λ's are different. Under these conditions phenotypic branching leading to polymorphisms can be observed even if the local and global dynamics are not chaotic. Moreover, there can be repeated branching, which leads to three instead of just two coexisting phenotypic branches. An example is shown in Figure 4a. Starting out from very low dispersal rates, the first branching occurs at a dispersal rate slightly lower than 0.2, and the upper branch then splits again at a dispersal rate of circa 0.8. The population dynamics are periodic during most of this evolutionary process, as is illustrated in Figure 4b. Nevertheless, the ecological dynamics change qualitatively and become more complicated as a consequence of the evolutionary dynamics of dispersal.

Branching like that shown in Figures 3 and 4a is reflected in invasion diagrams. The invasion diagram corresponding to Figure 4a is shown in Figure 4c, in which the resident-mutant pairs (d, d^{mut}) with $\rho(d, d^{mut}) > 0$ are again marked by a dot, while those with $\rho(d, d^{mut}) \leq 0$ are left blank. The boundary of the blank region consists of the "0-isoclines" of the invasion exponent, i.e., of those points (d, d^{mut}) with $\rho(d, d^{mut}) = 0$. This boundary has two parts, one being the diagonal (since $\rho(d, d) = 0$ for all d by definition), the other being a curve that intersects the diagonal at $(d, d^{mut}) \sim (0.2, 0.2)$. It is no coincidence that 0.2 is close to the first branching point in Figure 4a! The technical reason for branching can be best appreciated by considering a slightly more idealized version of the invasion diagram 4c, which is shown in Figure 5. Here the 0-isoclines of $\rho(d, d^{mut})$ consist of two straight lines (one again being the diagonal), which separate regions of positive and negative invasion exponents, and which intersect such that the angle they form in the positive regions is $> 90°$. This means that the resident value corresponding to the intersection point can be invaded by all mutant phenotypes.

Given such an invasion diagram, and assuming that invasion of a mutant implies extinction of the resident, the following evolutionary scenario will occur. Starting with a low dispersal resident phenotype X, only mutants with higher

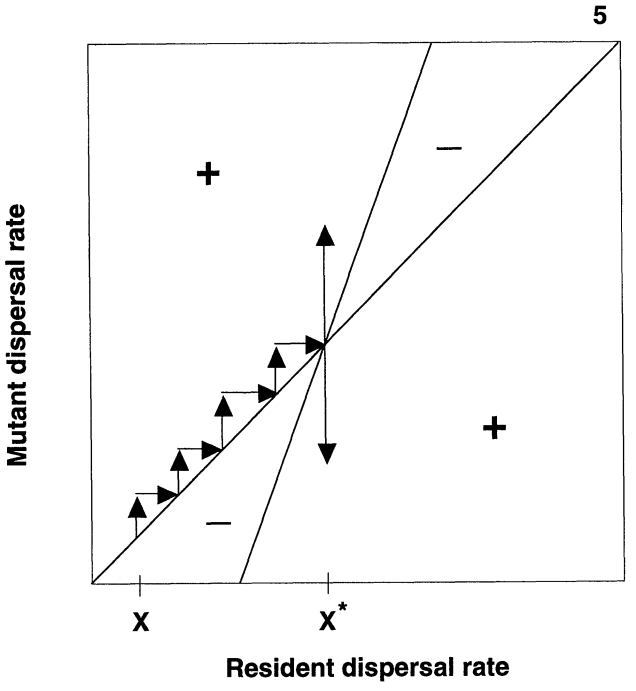

FIG. 5. Schematic invasion diagram corresponding to Figure 4c. In the regions marked by + the invasion exponent for a mutant-resident pair is positive, and the mutant can invade the corresponding resident. In regions marked by − invasion exponents are negative, indicating that invasion is impossible. On the solid lines invasion exponents are zero. Starting from a low value X, dispersal evolves to X^* as indicated by the arrows. Due to the relative position of the 0-isoclines, X^* can be invaded by both higher and lower mutants (indicated by vertical arrows), which results in evolutionary branching and polymorphic populations.

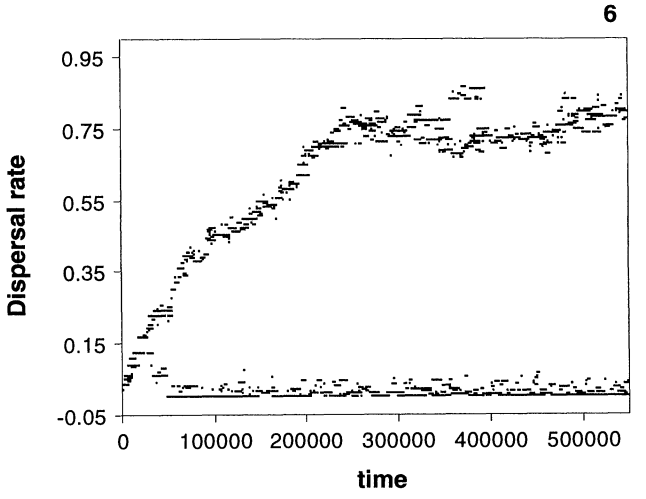

FIG. 6. Effects of noise. Same as Figure 4a, but with the deterministic fitness values in (14) replaced by Gaussian random variables with standard deviation equal to 12 percent of the deterministic means. The second branching of Figure 4a is lost because of the stochasticity.

dispersal can invade. Dispersal will therefore gradually evolve to higher values. The vertical arrows in Figure 5 indicate successful invasions, and the horizontal arrows indicate replacement of the resident by the invading mutants. A similar but opposite trajectory would result when starting out with very high dispersal residents. Clearly, in both cases the phenotype will reach the value X^*, corresponding to the intersection point of the 0-isoclines. However, due to the relative position of these isoclines, X^* can be invaded by both lower and higher dispersal mutants, as indicated by vertical arrows. Therefore, after having gradually evolved to X^*, the population will split into a polymorphism with coexisting phenotypic branches (Metz et al. 1996).

Even though the reality of the model may be more complicated than the schematic description of Figure 5 (e.g., invasion of a mutant may not cause immediate extinction of the resident), this is the basic scenario leading to the branching observed in Figures 3 and 4a. The example indicates how invasion exponents and invasion diagrams can be used to study evolutionary processes. Note, however, that the invasion diagrams used here only serve to detect whether branching occurs in a monomorphic population, but more information would be needed to determine the evolutionary dynamics beyond the initial branching. For example, the second branching event shown in Figure 4a cannot be detected by such diagrams, because at this point the resident is already polymorphic. See Metz et al. (1996) and Geritz et al. (1997) for a discussion of these points, as well as for possible biological interpretations of the 0-isoclines in invasion diagrams.

Based on our extensive numerical work we believe that the results presented in Figures 3 and 4 are typical for the evolution of dispersal in the unequal patch case: non-zero dispersal rates can be maintained as soon as local and global dynamics are not at a stable equilibrium, and evolutionary branching into two or three branches is possible under these conditions. (We have never observed more than three branches in our simulations.) In addition, branching can also be observed when there is noise in the system. For example, in Figure 6 we have introduced stochasticity in the system used for Figure 4a by assuming that the deterministic fitness values $f(\Sigma_{j=1}^{r} N_t^j)$ and $g(\Sigma_{j=1}^{r} M_t^j)$ in equation (14) are replaced by normally distributed random variables with mean the deterministic values and variance a certain proportion of the means. In the presence of noise a split into two phenotypic branches still occurs. However, if the noise level is large enough the second branching event of Figure 4a is lost, because stochasticity "cuts the edges" of the selection regime producing this polymorphism.

To conclude we again assume a cost to dispersal. Apart from generally lowering the evolutionarily stable dispersal rates, a cost can have the effect that phenotypic branches die out. An example is shown in Figure 7, which is the same as Figure 3, except that the basic metapopulation model (6) was replaced by system (15) with $s = 0.8$. The system "remembers" the branching that would occur without a cost (Fig. 3). However, due to the cost the high branch goes extinct some time after its appearance. When this happens, the lower branch starts to increase again (as would be predicted by considering the corresponding invasion diagram), until it reaches the branching point, and the process repeats itself. Similar to Figure 2b (but for different reasons), the result is evolutionary cycling in phenotype space of the lower branch,

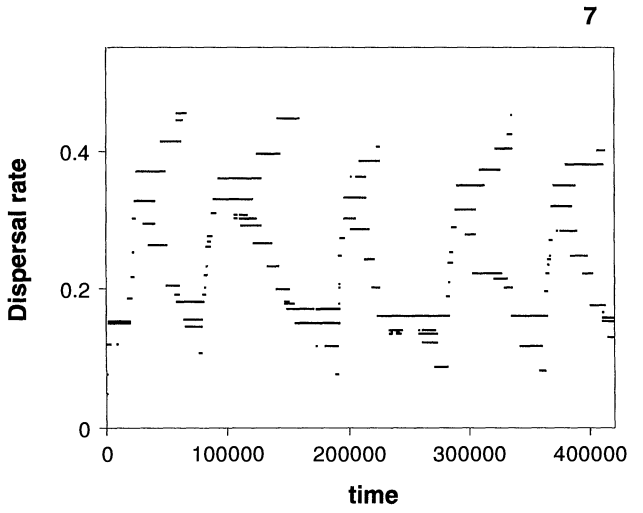

FIG. 7. Effects of a cost to dispersal on branching. This is the same as Figure 4a, except that $s = 0.8$ in system (15). Due to the cost, the upper dispersal branch dies out about 20,000 generations after it has appeared. This induces cyclic evolutionary dynamics of the lower branch (see text). The time resolution for the plot was 105 time steps.

with the additional feature of the repeated temporary appearance of a high dispersal phenotype.

DISCUSSION

We studied the evolution of dispersal rates in metapopulation models consisting of two patches with local dynamics given by difference equations. The local dynamics and the dispersal rate between the two patches determine the ecological dynamics of the metapopulation. For the evolution of dispersal rates, two basic ecological situations can be distinguished. If the metapopulation is at a stable equilibrium, then selection on dispersal is either neutral, which happens if the local populations sizes are equal, or selection leads to dispersal rates of zero, which occurs when the local abundances are different at the equilibrium.

In contrast, if the metapopulation exhibits non-equilibrium dynamics, non-zero dispersal rates can be maintained by selection (Figs. 1, 3, 4), and interesting evolutionary dynamics occur. Most notably, if the patches are ecologically different evolutionary branching into coexisting phenotypes can occur (Figs. 3, 4). Such branching can happen repeatedly, with three coexisting phenotypes at the evolutionary endpoint (Fig. 4). If the patches are ecologically identical, dispersal rates evolve to values inducing synchronous metapopulation dynamics. In this case, a cost to dispersal can produces non-equilibrium evolutionary dynamics, because different dispersal rates lead to qualitatively different population dynamic attractors in the metapopulation, which induce opposite selection pressures on dispersal. High dispersal rates lead to synchronized attractors, on which there is selection for lower dispersal rates if there is a cost to dispersal. In contrast, lower dispersal rates induce out-of-phase dynamics, which select for higher dispersal (Appendix). This interaction between ecological and evolutionary dynamics leads to evolutionary cycling in phenotype space (Fig. 2). Such cycling can also occur if a cost to dispersal is imposed on a system with evolutionary branching. Then, because of the cost the high dispersal branch dies out some time after its appearance through branching, the remaining low dispersal branch evolves back to the branching point, and the process repeats itself, leading to adaptive cycling (Fig. 7).

Our results are examples of non-equilibrium evolutionary dynamics and fit into the theory of adaptive dynamics proposed by Metz et al. (1996). Our work extends that of Holt and McPeek (1996), who concluded that non-zero dispersal rates can be maintained if the metapopulation dynamics are chaotic, and that two dispersal phenotypes could coexist in this case. Our results are different in that not only chaos, but any type of non-equilibrium dynamics can lead to the phenomena observed by Holt and McPeek (1996). The critical requirement for selection for non-zero dispersal rates is temporal as well as spatial heterogeneity in population size, which can be achieved by non-chaotic dynamics (but not with stable equilibrium dynamics). Also, we observed additional features such as evolutionary cycling and the occurrence of repeated branching with more than two coexisting phenotypes.

We note that the evolutionary cycling described here is different from that in Holt and McPeek (1996), in which different coexisting dispersal phenotypes merely fluctuate in the frequencies in which they occur in the population. These fluctuations occur over much shorter time scales than the evolutionary cycles in our examples (Figs. 2, 7), in which there is repeated occurrence and subsequent extinction of new phenotypes in the population. Nevertheless, fluctuations in the frequencies of different phenotypes do occur. Indeed, it may happen that a rare mutant is able to invade but subsequently goes extinct again, because invasion of the mutant induces a qualitative change in the dynamics of the metapopulation such that the new dynamic regime selects against the mutant (Doebeli 1997).

That a relatively small cost to dispersal can affect the evolutionary dynamics is apparent when comparing invasion diagrams with and without costs (Figs. 1, 2a): even a small cost to dispersal destroys the selectively neutral region of dispersal rates in the equal patch case. In fact, costs can have rather dramatic and counterintuitive effects for evolutionary dynamics, as the following example shows. If we consider dispersal phenotypes not as given by only one dispersal rate d, but by two different rates d_1 and d_2 describing dispersal from patch 1 to patch 2 and dispersal from patch 2 to patch 1 separately, we obtain a straightforward extension of the metapopulation model (6), and of the corresponding model with a cost to dispersal given by (15). Then the evolutionary dynamics take place in a two-dimensional phenotype space. In this case, it again often happens that without a cost to dispersal, there is branching into two different phenotypes, each given by two numbers (d_1, d_2). However, it can now happen that a cost to dispersal increases the number of coexisting branches from two to three. Figure 8 shows a system in which a cost leads to three branches, whereas no cost would lead to only two branches. Moreover, the three branches in Figure 8 occur simultaneously, i.e., there is a simultaneous split into three branches, instead of two successive splits with two branches each as in Figure 4a. The reason why a si-

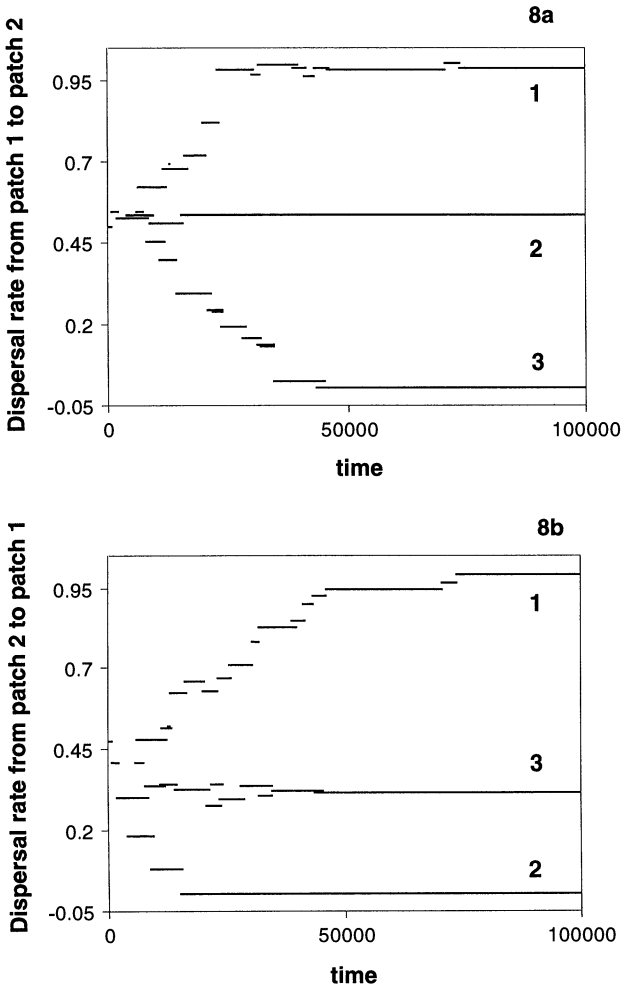

FIG. 8. Evolutionary branching in 2-dimensional phenotype space. This figure shows an example of a simultaneous split into three branches in the system with two dispersal rates d_1 and d_2 and a cost to dispersal that was the same for both directions of dispersal (s = 0.8). Figures 8a and 8b show the evolutionary dynamics of d_1 and d_2 respectively, with a time resolution of 25 time steps. Triple branching occurs around generation 10,000. The branches labeled with the same number in the two panels constitute one phenotype. At the evolutionary endpoint, the population consists of the dispersal phenotypes (1,1), (0.48,0.0), and (0.0,0.35). During the whole evolutionary transient the metapopulation exhibits simple 2- or 4-cyclic ecological dynamics (not shown). Without a cost, dispersal would split into only two branches (not shown). The parameters were a = 0.1, λ = 6, and b = 2.54 in patch 1; a = 0.1, λ = 18, and b = 2.54 in patch 2.

multaneous split into three branches is possible is that we assumed a two-dimensional phenotype space. In general, the number of branches into which a phenotypic lineage can split in one particular branching event is 1 + the dimension of phenotype space (Metz et al. 1996).

The models we used are very simple, but on general theoretical grounds evolutionary branching can be expected to occur in many other models as well (Metz et al. 1996, Geritz et al. 1997). For example, branching is likely if frequency dependence leads to changes in the distribution of a quantitative character such that the character mean evolves towards a fitness minimum, as in the predator-prey models of Abrams et al. (1993), or in Lotka-Volterra competition models with quantitative characters (Doebeli 1996). Technically, the only requirement for evolutionary branching is the existence of invasion diagrams which qualitatively look like Figure 5. These considerations lead us to believe that branching of the type observed in the present paper is of general evolutionary importance. Branching is a form of "phenotypic speciation," and it could be a fundamental mechanism underlying sympatric speciation. In sexual populations, however, recombination and segregation would lead to the constant production of phenotypes that are intermediate between the branches, which would prevent speciation. To overcome this problem, there must be evolution of assortative mating, e.g., because intermediates have a selective disadvantage. For example, if there is branching into one very low dispersal rate and one very high dispersal rate, the difference in dispersal behavior could be reflected in morphological differences (e.g., wings) on which assortative mating could be based. Another possibility is that the low- and high-dispersal phenotypes evolve different reproductive timings within the season, which would again lead to assortative mating. Several recent empirical and theoretical studies suggest that sympatric speciation is more common than generally believed (Schluter 1994; Schliewen et al. 1994; Feder 1995; Johnson et al. 1996; Doebeli 1996; Kawecki 1996), and combining models for evolutionary branching with population genetic models for assortative mating promises to yield more insights into the mechanisms and processes of sympatric speciation.

There are many other possible extensions of the simple metapopulation models considered here. For example, one could consider models with more than two patches, and models in which dispersal is not given by constant rates, but by density-dependent rates. Jánosi and Scheuring (1997) considered metapopulations in which dispersal occurs when the local population density in a patch reaches a certain threshold. In their model, more mobile phenotypes have a selective advantage if there is temporal and spatial variation in population abundance. Moreover, Jánosi and Scheuring (1997) argue that the evolutionary stable dispersal strategies prevent chaotic metapopulation dynamics, which relates to another problem that deserves close inspection: the evolution of the population dynamics as a consequence of the evolution of dispersal. In our model sudden changes in the ecological dynamics occur during the long evolutionary transients, and the evolution of dispersal rates often leads to more complicated population dynamics (Fig. 4). Thus, the ecological metapopulation dynamics influence the evolutionary dynamics of dispersal rates, and the evolutionary change in dispersal rates feeds back to induce changes in the ecological dynamics. Clearly, the work presented here is at most a preliminary step towards understanding the details of this interaction and its implications for ecological complexity and speciation.

ACKNOWLEDGEMENTS

We thank R. Holt, M. Gyllenberg, and an anonymous referee for very helpful comments and suggestions.

LITERATURE CITED

ABRAMS, P. A., H. MATSUDA, AND Y. HARADA. 1993. Evolutionary unstable fitness maxima and stable fitness minima of continuous traits. Evol. Ecol. 7:465–487.

BELLOWS, T. S., JR. 1981. The descriptive properties of some models for density dependence. J. Anim. Ecol. 50:139–156.
BLARER, A., AND M. DOEBELI. 1996. In the red zone. Nature 380: 589–590.
CRESSMAN, R. 1992. The stability concept of evolutionary game theory. Lect. Notes Biomath. 94. Springer, Berlin, Germany.
DOEBELI, M. 1995. Dispersal and dynamics. Theor. Popul. Biol. 47:82–106.
———. 1996. A quantitative genetic competition model for sympatric speciation. J. Evol. Biol. 9:893–909.
———. 1997. Invasion of rare mutants does not imply their evolutionary success: a counterexample from metapopulation theory. J. Evol. Biol. *In press.*
FEDER, J. L. 1995. The effects of parasitoids on sympatric host races of *Rhagoletis pomonella* (Diptera: Tephritidae). Ecology 76:801–813.
GERITZ, S. A. H., F. J. A. JACOBS, J. S. VAN HEERWAARDEN, E. KISDI, G. MESZÉNA, AND J. A. J. METZ. 1997. Evolutionarily singular strategies and the adaptive growth and branching of the evolutionary tree. Evol. Ecol. *In press.*
GYLLENBERG, M., G. SÖDERBACKA, AND S. ERICSSON. 1993. Does migration stabilize local population dynamics? Analysis of a discrete metapopulation model. Math. Biosci. 118:25–49.
HASSELL, M. P. 1975. Density-dependence in single-species models. J. Anim. Ecol. 44:283–296.
HASTINGS, A. 1983. Can spatial variation alone lead to selection for dispersal? Theor. Popul. Biol. 24:244–251.
———. 1993. Complex interactions between dispersal and dynamics: lessons from coupled logistic equations. Ecology 74:1362–1372.
HOLT, R. D. 1985. Population dynamics in two-patch environments: some anomalous consequences of an optimal habitat distribution. Theor. Popul. Biol. 28:181–208.
HOLT, R. D., AND M. A. MCPEEK. 1996. Chaotic population dynamics favors the evolution of dispersal. Am. Nat. 148:709–718.
JÁNOSI, I. M., AND I. SCHEURING. 1997. On the evolution of density dependent dispersal in a spatially structured population model. J. theor. Biol. 187:397–408.
JOHNSON, P. A., F. C. HOPPENSTAEDT, J. J. SMITH, AND G. L. BUSH. 1996. Conditions for sympatric speciation: a diploid model incorporating habitat fidelity and non-habitat assortative mating. Evol. Ecol. 10:187–205.
KAWECKI, T. J. 1996. Sympatric speciation driven by beneficial mutations. Proc. R. Soc. Lond. B. 263:1515–1520.
LLOYD, A. L. 1995. The coupled Logistic map—a simple model for the effects of spatial heterogeneity on population dynamics. J. theor. Biol. 173:217–230.
MAY, R. M., AND G. F. OSTER. 1976. Bifurcations and dynamic complexity in simple ecological models. Am. Nat. 110:573–599.
MAYNARD SMITH, J. 1982. Evolution and the theory of games. Cambridge Univ. Press, Cambridge, U.K.
MAYNARD SMITH, J., AND M. SLATKIN. 1973. The stability of predator–prey systems. Ecology 54:384–391.
MCPEEK, M. A., AND R. D. HOLT. 1992. The evolution of dispersal in spatially and temporally varying environments. Am. Nat. 140: 1010–1027.
METZ, J. A. J., R. M. NISBET, AND S. A. H. GERITZ. 1992. How should we define 'fitness' for general ecological scenarios? Trends Ecol. Evol. 7:198–202.
METZ, J. A. J., S. A. H. GERITZ, G. MESZÉNA, F. J. A. JACOBS, AND J. S. VAN HEERWAARDEN. 1996. Adaptive dynamics: a geometrical study of the consequences of nearly faithful reproduction. Pp. 183–231 *in* S. J. van Strien and S. M. Verduyn Lunel, eds. Stochastic and spatial structures of dynamical systems. North Holland, Amsterdam, The Netherlands.
RAND, D. A., H. B. WILSON, AND J. M. MCGLADE. 1994. Dynamics and evolution: evolutionary stable attractors, invasion exponents and phenotype dynamics. Philos. Trans. R. Soc. Lond. B 343: 261–283.
RICKER, W. E. 1954. Stock and recruitment. J. Fish. Res. Board Can. 11:559–623.
ROFF, D. A. 1992. The evolution of life histories. Chapman and Hall, London.
ROHANI, P., R. M. MAY, AND M. P. HASSELL. 1996. Metapopulations and equilibrium stability—the effects of spatial structure. J. theor. Biol. 181:97–109.
SCHLIEWEN, U. K., D. TAUTZ, AND S. PÄÄBO. 1994. Sympatric speciation suggested by monophyly of Crater Lake cichlids. Nature 368:629–632.
SCHLUTER, D. 1994. Experimental evidence that competition promotes divergence in adaptive radiation. Science 266:798–801.
STEARNS, S. C. 1992. The evolution of life histories. Oxford Univ. Press, Oxford.

Corresponding Editor: E. Martins

APPENDIX

Here we prove that a resident whose metapopulation dynamics are given by an out-of-phase 2-cycle (Hastings 1993) can be invaded by nearby mutants if and only if the mutant dispersal rate is higher than that of the resident. An out-of-phase 2-cycle is characterized by two densities P and Q such that the metapopulation density vector $\binom{N_1}{N_2}$ alternates between $\binom{P}{Q}$ and $\binom{Q}{P}$. Thus the time series of the resident looks like $\binom{P}{Q} \to \binom{Q}{P} \to \binom{P}{Q} \to \ldots$. Let d_r be the dispersal rate of the resident, and let $p = f(P)$ and $q = f(Q)$ be the fitness values corresponding to the densities in the two local patches. (Note that the ensuing arguments are independent of the particular form of the fitness function in model (1)). Then the transition matrix from $\binom{P}{Q}$ to $\binom{Q}{P}$ is given by

$$X = \begin{pmatrix} (1 - d_r)p & d_r q \\ d_r p & (1 - d_r)q \end{pmatrix}, \tag{A1}$$

and that from $\binom{Q}{P}$ to $\binom{P}{Q}$ by

$$Y = \begin{pmatrix} (1 - d_r)q & d_r p \\ d_r q & (1 - d_r)p \end{pmatrix}. \tag{A2}$$

Then, since we are on a 2-cycle,

$$\begin{pmatrix} P \\ Q \end{pmatrix} = Y \cdot X \cdot \begin{pmatrix} P \\ Q \end{pmatrix},$$

where

$$Y \cdot X = \begin{pmatrix} pq(1 - d_r)^2 + p^2 d_r^2 & (pq + q^2)(1 - d_r)d_r \\ (pq + p^2)(1 - d_r)d_r & pq(1 - d_r)^2 + q^2 d_r^2 \end{pmatrix}. \tag{A3}$$

Let J denote the dominant eigenvalue of this matrix. Then J is the geometric mean fitness over two generations. Hence $J = 1$, since $\binom{P}{Q}$ is a stable equilibrium point for the 2-step dynamics given by $Y \cdot X$, so that the modulus of the other eigenvalue is smaller than 1. To determine the selection pressure on the dispersal rate, we have to calculate the derivative of the dominant eigenvalue J with respect to the dispersal rate and evaluate it at the resident dispersal rate. When doing this, we can treat the quantities $p = f(P)$ and $q = f(Q)$ as fixed parameters, since the mutant is initially rare and has no influence on the population dynamics given by the resident out-of-phase 2-cycle. Our claim that such cycles induce selection for higher dispersal rates follows from the next

Proposition:

$$\frac{\partial J}{\partial d}(d_r) > 0,$$

that is, higher dispersal rates than that of the resident will lead to a higher dominant eigenvalue of the two-step transition matrix, and hence rare mutants with higher dispersal rates have a long-term growth rate that is larger than 1.

Proof: Let us first consider the one step transition of the resident, from which we will extract some useful information. This transition is given by

$$\begin{pmatrix} Q \\ P \end{pmatrix} = X \cdot \begin{pmatrix} P \\ Q \end{pmatrix}, \tag{A4}$$

i.e.,

$$Q = (1 - d_r)pP + d_r qQ$$

$$P = d_r pP + (1 - d_r)qQ. \tag{A5}$$

Adding the two equations in (A5) yields $P + Q = pP + qQ$, and hence

$$P = Q \cdot \frac{q - 1}{1 - p}. \tag{A6}$$

Since $P, Q > 0$, this implies that not both p and q are simultaneously < 1 or > 1. Without restriction, we assume that $p < 1$ and $q > 1$. Since $p = f(P)$, this implies that P is above the carrying capacity of the local populations, and similarly, Q is below the carrying capacity. In particular, $P > Q$. From this we conclude from (A6) that $(q - 1)/(1 - p) > 1$, i.e., that

$$p + q - 2 > 0. \tag{A7}$$

We now derive an expression for d_r as a function of p and q. Inserting (A6) into the first equation of (A5) we obtain

$$Q = (1 - d_r)p \cdot \frac{q - 1}{1 - p} Q + d_r qQ$$

$$= Q \cdot \left[(1 - d_r)p \frac{q - 1}{1 - p} + d_r q \right]. \tag{A8}$$

It follows that $(1 - d_r)p(q - 1)/(1 - p) + d_r q = 1$, and after some rearranging that

$$d_r = \frac{1 - pq}{p + q - 2pq}. \tag{A9}$$

Moreover, from $(q - 1)(p - 1) < 0$ we see that $pq - p - q + 1 < 0$, hence that

$$p + q - 2pq > 1 - pq, \tag{A10}$$

and since $0 \le d_r \le 1$, it follows from (A9) that the right hand side of (A10) is ≥ 0, and hence that

$$p + q - 2pq > 0. \tag{A11}$$

After these preparations, we now calculate the derivative of the dominant eigenvalue $J(d)$. From (A3), standard procedures lead to the two eigenvalues of $Y \cdot X$ as functions of the dispersal rate d being

$$x_{1,2} = pq(1 - d)^2 + \frac{(p^2 + q^2)}{2} d^2 \pm \frac{1}{2} \sqrt{(p + q)^2 d^2 [4pq(1 - 2d) + (p + q)^2 d^2]}. \tag{A12}$$

Since $pq(1 - d)^2 + (p^2 + q^2)d^2/2 > 0$, the dominant eigenvalue $J(d)$ is

$$J(d) = pq(1 - d)^2 + \frac{(p^2 + q^2)}{2} d^2 + \frac{1}{2} \sqrt{(p + q)^2 d^2 [4pq(1 - 2d) + (p + q)^2 d^2]}. \tag{A13}$$

For the resident dispersal rate d_r we have $J(d_r) = 1$, and it follows from (A13) that

$$\sqrt{(p + q)^2 d_r^2 [4pq(1 - 2d_r) + (p + q)^2 d_r^2]} = 2 - 2pq(1 - d_r)^2 - (p^2 + q^2)d_r^2. \tag{A14}$$

Now, taking the derivative of $J(d)$ with respect to d yields

$$\frac{\partial J}{\partial d}(d) = -2pq(1 - d) + (p^2 + q^2)d + \frac{2(p + q)^2 d[4pq(1 - 2d) + (p + q)^2 d^2]}{4\sqrt{(p + q)^2 d^2 [4pq(1 - 2d) + (p + q)^2 d^2]}} + \frac{(p + q)^2 d^2 [-8pq + 2d(p + q)^2]}{4\sqrt{(p + q)^2 d^2 [4pq(1 - 2d) + (p + q)^2 d^2]}}. \tag{A15}$$

Using (A9) for d_r, and (A14) for the value of the square root at d_r, we get after some algebra that is most easily done using a program for symbolic mathematics:

$$\frac{\partial J}{\partial d}(d_r) = \frac{2(p + q - 2pq)^2}{p + q - 4pq + p^2 q + pq^2}. \tag{A16}$$

By (A11), the nominator of this equation is > 0. The denominator can be written as a sum

$$p + q - 4pq + p^2 q + pq^2 = (p + q - 2pq) + pq(p + q - 2). \tag{A17}$$

By (A11) and (A7) both summands on the right hand side of (A17) are > 0, which completes the proof.